Forced vibrations of a cantilever beam

Article *in* European Journal of Physics · September 2012

DOI: 10.1088/0143-0807/33/5/1187

3 authors:

C. E. Repetto
Instituto de Física Rosario (UNR-CONICET)

A. Roatta
Instituto de Física Rosario

Reinaldo Welti
Rosario National University

Forced vibrations of a cantilever beam

2012 Eur. J. Phys. 33 1187

(http://iopscience.iop.org/0143-0807/33/5/1187)

IOP Publishing European Journal of Physics
Eur. J. Phys. **33** (2012) 1187–1195 doi:10.1088/0143-0807/33/5/1187

Forced vibrations of a cantilever beam

C E Repetto[1,2], A Roatta[1,2] and R J Welti[1]

[1] Laboratorio de Vibraciones y Ondas, Departamento de Fisica y Química, Escuela de Formación Básica, Facultad de Ciencias Exactas, Ingeniería y Agrimensura (UNR), Pellegrini 250, S2000BTP Rosario, Argentina
[2] Instituto de Física Rosario (CONICET-UNR), Bv 27 de febrero 210 bis, S2000EZP Rosario, Argentina

E-mail: welti@fceia.unr.edu.ar

Received 24 April 2012, in final form 11 June 2012
Published 9 July 2012
Online at stacks.iop.org/EJP/33/1187

Abstract
The theoretical and experimental solutions for vibrations of a vertical-oriented, prismatic, thin cantilever beam are studied. The beam orientation is 'downwards', i.e. the clamped end is above the free end, and it is subjected to a transverse movement at a selected frequency. Both the behaviour of the device driver and the beam's weak-damping resonance response are compared for the case of an elastic beam made from PVC plastic excited over a frequency range from 1 to 30 Hz. The current analysis predicts the presence of 'pseudo-nodes' in the normal modes of oscillation. It is important to note that our results were obtained using very simple equipment, present in the teaching laboratory.

(Some figures may appear in colour only in the online journal)

1. Introduction

Experimental techniques, such as free-vibration decay, forced vibration, rotating-beam deflection and pulse propagation, have been widely used to measure the dynamic elastic modulus and damping of materials. These methods are now accompanied by numerical simulations, which play an important role in modern vibration analysis. These solutions give reliable answers if the experiments have practical problems, are too expensive or it is impossible to analyse the problem with analytical methods [1–4].

In particular, models based on beam-like elements, with different boundary conditions, can be used to simulate the response of structures in engineering applications. For example, we can model the vibrational response of spacecraft antennae, robot arms, building components, bridge structures and parts of musical instruments.

Vibration analysis and the presence of resonance are important factors in engineering education, since they can lead to the failure of structures or to noise production [5].

In this paper we study the relationship between natural frequencies and vibrational modes of a bounded elastic system and the related resonance phenomena. From the educational point of view, we employ a simple system to show the possibility of characterizing a material at an introductory level to facilitate the student's understanding.

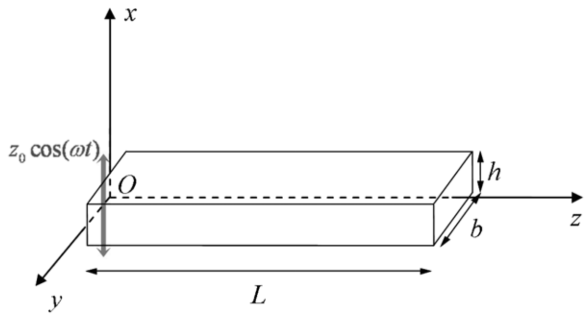

Figure 1. Diagram of the cantilever beam studied.

The paper is organized as follows. First, we present the mathematical solutions for forced oscillations of a cantilever beam, with an emphasis on analysing the beam's behaviour near resonance. Second, we compare experimental and numerical results for forced oscillations of a rectangular plastic beam. Here we pay special attention to explaining the amplitude of the resonance peak and in evaluating the effect of gravity on the calculated resonant frequencies. Finally, we present our conclusions.

2. The equation of motion for a cantilever beam

We consider the cantilever-beam geometry shown in figure 1, where the end $z = 0$ is connected to a device driver that oscillates with amplitude z_0 and frequency ω. The other end of the beam, $z = L$, is free to vibrate. The model assumes that the beam is uniform along its length, with a constant cross-sectional area. In addition, we assume that the beam material is linear elastic, isotropic and homogeneous. Also, the beam is taken to be much longer than it is wide. In this case, the vibrations of the beam can be described by the Euler–Bernoulli equation [6–10]

$$\frac{EI}{\rho S}\frac{\partial^4 u(z,t)}{\partial z^4} + \frac{\partial^2 u(z,t)}{\partial t^2} + \gamma\frac{\partial u(z,t)}{\partial t} = 0, \tag{2.1}$$

where $I(z)$ (m^4) is the second moment of inertia of the cross section with respect to its longitudinal axis, E (N m^{-2}) is Young's modulus, ρ (Kg m^{-3}) is the mass density of the beam, $S(z)$ (m^2) is the cross section, γ (s^{-1}) is the damping coefficient, L (m) is the length of the beam and $u(z,t)$ (m) represents the displacement of the beam corresponding to the position z (m) at a time t (s).

The first two boundary conditions on the forced end of the beam, $z = 0$, are taken as

$$u(0,t) = z_0 e^{i\omega t} \quad (a), \qquad \frac{\partial u(0,t)}{\partial z} = 0 \quad (b), \tag{2.2}$$

while the second two boundary conditions, at $z = L$, specify that the bending moment and shearing forces on the free end of the beam are zero at all times [11]:

$$\frac{\partial^2 u(L,t)}{\partial z^2} = 0 \quad (c), \qquad \frac{\partial^3 u(L,t)}{\partial z^3} = 0 \quad (d). \tag{2.3}$$

In order to determine the beam's movement, an initial deflection and a velocity are imposed along the z axis,

$$u(z,0) = F(z), \qquad \frac{\partial u}{\partial t}(z,0) = G(z). \tag{2.4}$$

Finally, the Euler–Bernoulli equation (2.1) is solved with boundary conditions (2.2) and (2.3) and initial conditions (2.4).

3. Solution of the forced beam equation

The displacement $u(z,t)$ of any point of the beam must satisfy equation (2.1) and, in the permanent regime, any point of the beam oscillates with the excitation frequency ω. Therefore,

$$\widehat{u}(z,t) = Z(z)\,\mathrm{e}^{\mathrm{i}\omega t}, \tag{3.1}$$

where $u(z,t) = \mathrm{Re}(\hat{u}(z,t))$.

Substituting equation (3.1) into (2.1)—the Euler–Bernoulli equation—we find that the Z function must satisfy the following differential equation:

$$\frac{\mathrm{d}^4 Z}{\mathrm{d}z^4} - q^4 Z = 0, \tag{3.2}$$

where

$$q^4 = \frac{\omega^2}{c^2}\left(1 - \mathrm{i}\frac{\gamma}{\omega}\right) \tag{3.3}$$

and $c^2 = \frac{EI}{\rho S}$. We observe that q^4 is a parameter that depends on the external frequency ω through (3.3), and ω can take any real value.

The boundary conditions to solve equation (3.2) are as follows:

$$\begin{aligned} &Z(0) = z_0, \quad \frac{\mathrm{d}Z}{\mathrm{d}z}(0) = 0 \quad (a),\\ &\frac{\mathrm{d}^2 Z}{\mathrm{d}z^2}(L) = 0, \quad \frac{\mathrm{d}^3 Z}{\mathrm{d}z^3}(L) = 0 \quad (b). \end{aligned} \tag{3.4}$$

The general solution of (3.2) is

$$Z(z) = c_1 \cosh qz + c_2 \sinh qz + c_3 \cos qz + c_4 \sin qz, \tag{3.5}$$

where c_1, c_2, c_3 and c_4 are constants of integration to be determined by the boundary conditions. From the conditions at $x = 0$, (3.4)(a), we find that $c_3 = -c_1 + z_0$ and $c_4 = -c_2$.

The last condition, (3.4)(b), requires that c_1 and c_2 satisfy

$$\begin{pmatrix} \cosh qL + \cos qL & \sinh qL + \sin qL \\ \sinh qL - \sin qL & \cosh qL + \cos qL \end{pmatrix} \begin{pmatrix} c_1 \\ c_2 \end{pmatrix} = \begin{pmatrix} z_0 \cos qL \\ -z_0 \sin qL \end{pmatrix}. \tag{3.6}$$

Solving, we obtain

$$\left.\begin{aligned} c_1 &= z_0 \frac{\cosh qL \cos qL + \sinh qL \sin qL + 1}{\Delta} \\ c_2 &= -z_0 \frac{\cosh qL \sin qL + \sinh qL \cos qL}{\Delta} \end{aligned}\right\}, \tag{3.7}$$

where

$$\Delta = 2(1 + \cosh qL \cos qL). \tag{3.8}$$

Substituting the values of c_i $(i = 1, 2, 3, 4)$ into (3.5), we find

$$\begin{aligned} Z(z) = {} & z_0 \frac{\cosh qL \cos qL + \sinh qL \sin qL + 1}{\Delta} (\cosh qz - \cos qz) \\ & - z_0 \frac{\cosh qL \sin qL + \sinh qL \cos qL}{\Delta} (\sinh qz - \sin qz) + z_0 \cos qz. \end{aligned} \tag{3.9}$$

Finally, the solution of the problem is

$$u(z,t) = \mathrm{Re}(\hat{u}(z,t)) = \mathrm{Re}(Z(z)\,\mathrm{e}^{\mathrm{i}\omega t}). \tag{3.10}$$

It can be seen that when (3.8) equals zero, we obtain the eigenfrequencies of the problem associated with the free oscillations of a cantilever [6, 11]:

$$\hat{\omega}_n = \mathrm{i}\frac{\gamma}{2} \pm \sqrt{\omega_n^2 - \frac{\gamma^2}{4}}, \tag{3.11}$$

where

$$\omega_n = \frac{\mu_n^2}{L^2}c \tag{3.12}$$

and $\mu_1 = 1.875, \quad \mu_2 = 4.694, \quad \mu_n \approx (2n-1)\pi/2$ with $n \geqslant 3$.

4. Oscillations of the beam in the proximity of a resonance

The oscillation amplitude, A, of the free end of the beam, $z = L$, is given by

$$A(\omega) = |Z(L)| = \left|\frac{2z_0}{\Delta}(\cos qL + \cosh qL)\right|. \tag{4.1}$$

The complex parameter q in (3.3) can be split up into a real and an imaginary part, $q = \alpha - \mathrm{i}\beta$, where $\alpha = \sqrt{\omega/c}$ and $\beta = \alpha\gamma/4\omega$.

When $\beta \ll 1$, we can write

$$\begin{aligned} \cos qL &= \cos(\alpha - \mathrm{i}\beta)L \approx \cos\alpha L + (\mathrm{i}\beta L)\sin\alpha L \\ \cosh qL &= \cosh(\alpha - \mathrm{i}\beta)L \approx \cosh\alpha L - (\mathrm{i}\beta L)\sinh\alpha L. \end{aligned} \tag{4.2}$$

Substituting into (3.8), we obtain

$$\Delta \approx 2\,[1 + F(\alpha L) + \mathrm{i}\beta L G(\alpha L)], \tag{4.3}$$

where

$$\begin{aligned} F(\alpha L) &= \cos(\alpha L)\cosh(\alpha L) \\ G(\alpha L) &= \sin(\alpha L)\cosh(\alpha L) - \cos(\alpha L)\sinh(\alpha L). \end{aligned} \tag{4.4}$$

Considering that the damping is weak, $\gamma \ll \omega_n$, recalling from (3.8) that in the proximity of a resonance, $\omega \approx \omega_n$, $\cos\mu_n = -\cosh^{-1}\mu_n$, and expanding F and G into Taylor's series up to first order, it can be shown that the determinant, Δ, can be approximated by

$$\Delta \approx \frac{\mu_n}{\omega_n}G(\mu_n)\left[-(\omega - \omega_n) + \mathrm{i}\frac{\gamma}{2}\right]. \tag{4.5}$$

Thus, the modulus of Δ is given by

$$|\Delta| = \frac{\mu_n}{\omega_n}|G(\mu_n)|\left[(\omega - \omega_n)^2 + \frac{\gamma^2}{4}\right]^{1/2}. \tag{4.6}$$

It must be noted that in these equations, ω_n is the nth-natural frequency of the beam oscillations in the absence of damping. Hence,

$$A(\omega) \approx 2z_0\,\omega_n \frac{|\cos qL + \cosh qL|}{\mu_n|G(\mu_n)|\left[(\omega - \omega_n)^2 + \frac{\gamma^2}{4}\right]^{1/2}}. \tag{4.7}$$

In order to predict the behaviour of resonant amplitude, we proceed similarly in the numerator of (4.1); finally, we obtain

$$A(\omega = \omega_n) \approx 4\frac{z_0}{\gamma L}\frac{\omega_n^{1/2}}{(\rho S/\mathrm{EI})^{1/4}}. \tag{4.8}$$

If z_0 and γ are not functions of ω_n, we conclude that $A(\omega = \omega_n)$, in the neighbourhood of resonance, grows in proportion to the square root of ω_n. In the following section, this behaviour will be discussed.

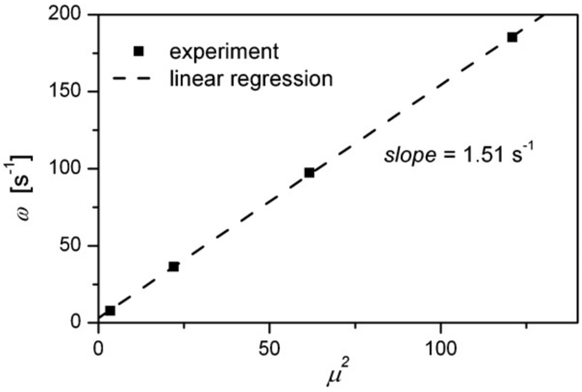

Figure 2. Measured resonance frequencies of the first four normal modes of oscillations of the beam.

Table 1. Comparison between measured and theoretical resonance frequencies.

Angular frequency (s^{-1})	
Experimental	Theoretical ($\gamma = 2\,s^{-1}$)
7.79	5.2
36.44	33.2
97.39	93
185.35	182.3

5. Experimental and theoretical results

A thin plastic strip was oriented 'downwards' with the upper end clamped to a wave driver and the other free. The driver imposes a transverse displacement at a selected frequency at the point $z = 0$ of the beam. The length of the cantilevered strip is $L = 0.502$ m, and the cross-sectional dimensions are $h = 0.89$ mm and $b = 1.7$ mm (see figure 1).

The measured resonance frequencies of the first four normal modes of oscillation of the beam are plotted versus μ_n^2 in figure 2. A linear fit of these measurements satisfies the behaviour described by equation (3.12).

Knowing that $I(z) = bh^3/12$ and substituting the appropriate values for b and h, we obtain the value $c = 0.38$ m^2 s^{-1}. With this measurement and the handbook value of $\rho = 1420$ Kg m^{-3} for PVC, we can estimate a Young's modulus of $E = 3.1 \times 10^9$ Pa, which is consistent for this material [12].

The oscillation amplitude as a function of frequency of the beam's free end is evaluated with equation (4.1) using $\gamma = 2\,s^{-1}$. This coefficient represents a weak damping in all the modes except the fundamental one. Figure 3 shows the theoretical amplitude $Z(L)$ versus ω, where the vertical axis is in z_0 units. In addition, we plot the approximate expression for the maximum displacement in the proximity of resonance, (4.8). It can be seen that the predicted growth of the peak amplitude is well described as proportional to the square root of the resonant frequency. On the other hand, the peaks' positions give us the predicted resonant frequencies of the system. Table 1 shows a comparison between the measured resonance frequencies and the theoretical ones. It should be noted that, with the exception of the fundamental mode, the discrepancies between the experimental and calculated results are less than 9%. If we

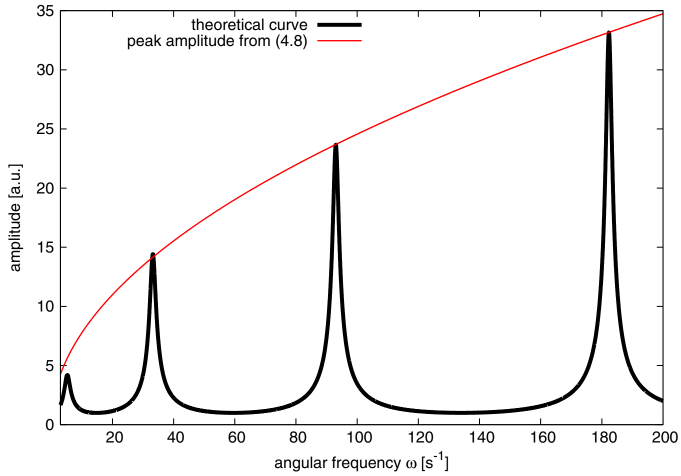

Figure 3. Amplitude of the free end of the beam $Z(L)$ versus ω.

increase γ from 0.01 to 10 s^{-1}, all the resonance peaks broaden, and only the frequency of the fundamental mode changes significantly. For example, $\omega_{res} = 5.3\ s^{-1}$ for $\gamma = 0.01\ s^{-1}$ and $\omega_{res} = 2.8\ s^{-1}$ for $\gamma = 10\ s^{-1}$. For the latter case, the peak's maximum is slightly greater than z_0. In all cases, we find that the theoretical frequencies are less than the experimental ones. The effect of gravity on the vibration of vertical cantilevers can explain the differences between the experimental and predicted resonant frequencies, especially for the first mode.

Virgin *et al* [13] consider the free vibration of vertical-oriented thin, prismatic beams in the absence of damping and they conclude that the dynamic response is different according to whether the fixed end of the beam is the lower or upper end. As they explain, in the former case the natural frequencies are reduced due to the compressive nature of the self-weight loading. Unlike in the latter case, the frequencies increase due to the stiffening effect of the beam weight. Based on the paper of Virgin *et al* [13], we calculate a non-dimensional coefficient $\alpha = -WL^2/EI$, where W is the weight of the beam, which reflects both the orientation (in terms of its sign) and the influence of bending versus gravity (in terms of its magnitude). The case $\alpha = 0$ corresponds to a gravity-free system (in practice, a short horizontal cantilever), while $\alpha > 0$ and $\alpha < 0$ correspond to the 'up' and 'down' configurations, respectively. For our experimental system, we found a value of $\alpha = -8.58$, which explains why, if the effect of gravity is not considered, the measured value of the fundamental-mode frequency is greater than the predicted one. Furthermore, it is shown by Virgin *et al* [13] that the influence of the α parameter decreases as the system oscillates at greater natural frequencies. This too can be observed in table 1. While the experimental value remains above the theoretical, the difference between the two decreases as the frequency increases.

To check the validity of the approximation in the proximity of resonance, figure 4 shows plots of both equations (4.1) and (4.7) around the first two resonant frequencies. We observe a good fit that improves in the higher modes.

With respect to the displacement of the free end of the beam, in our experiment we did not observe the predicted growth of peak amplitude (as the square root of ω_n, (4.8) and figure 3). It is possible that the shaker amplitude z_0 at the clamped end of the beam is not constant for the different resonant frequencies, producing this effect.

To test this hypothesis, we mounted a rod connected to a loudspeaker's membrane to the shaker. If we assume that this device gives a constant power, then $z_0\omega =$ constant. Figure 5

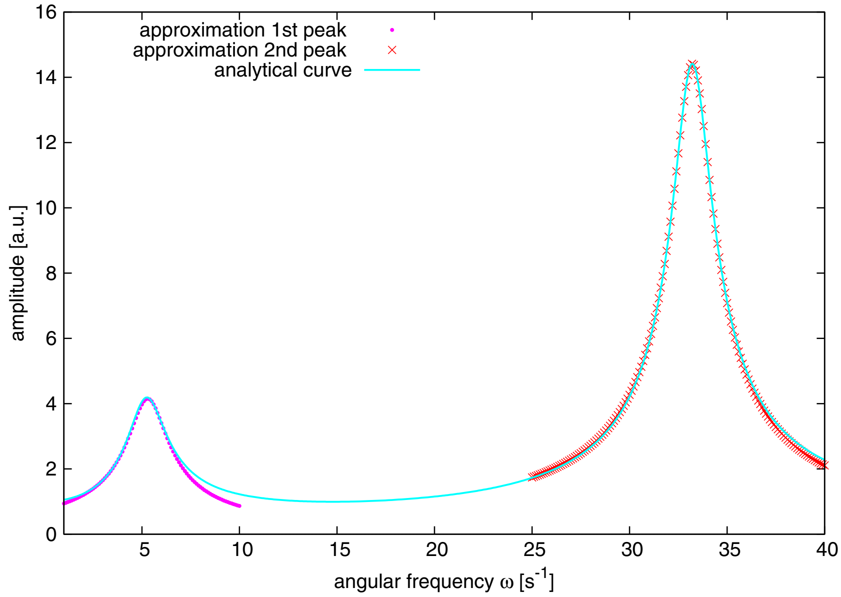

Figure 4. Analytical curve for the amplitude of the free end of the beam $Z(L)$ versus ω, and approximations (4.7) around the first two resonant frequencies.

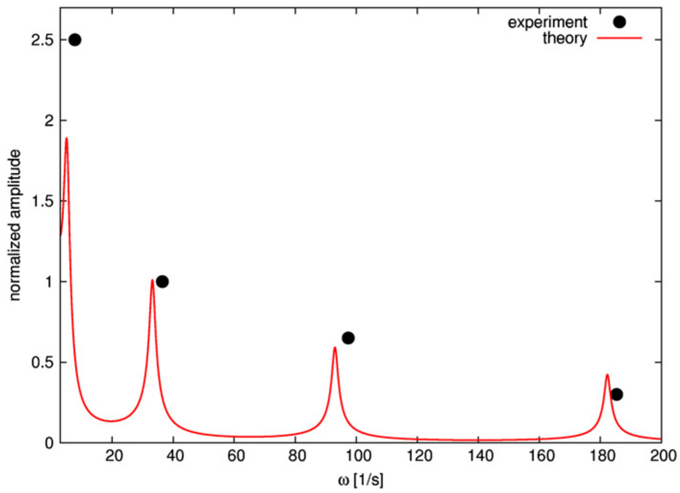

Figure 5. Experimental and theoretical normalized amplitude of the free end of the beam $Z(L)$ versus ω. Theoretical results satisfy the restriction $z_0\omega$ = constant for the clamped end.

shows the comparison between the amplitude of the free end of the beam $Z(L)$ versus ω for the case where the clamped end satisfies the constant-power restriction and the measured amplitudes at the resonant frequencies. The results were normalized by the second-mode amplitude because, as explained in the previous paragraph, this mode is more reliable than the first. The agreement between experimental and predicted values validates the constant-power hypothesis.

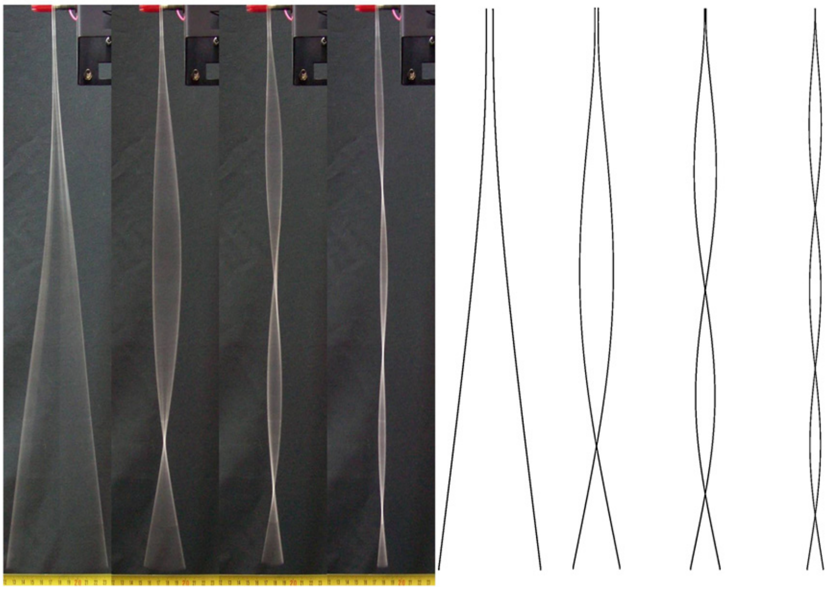

Figure 6. Four first modes of a vertical-oriented plastic beam. Left: photographs; right: theoretical solutions.

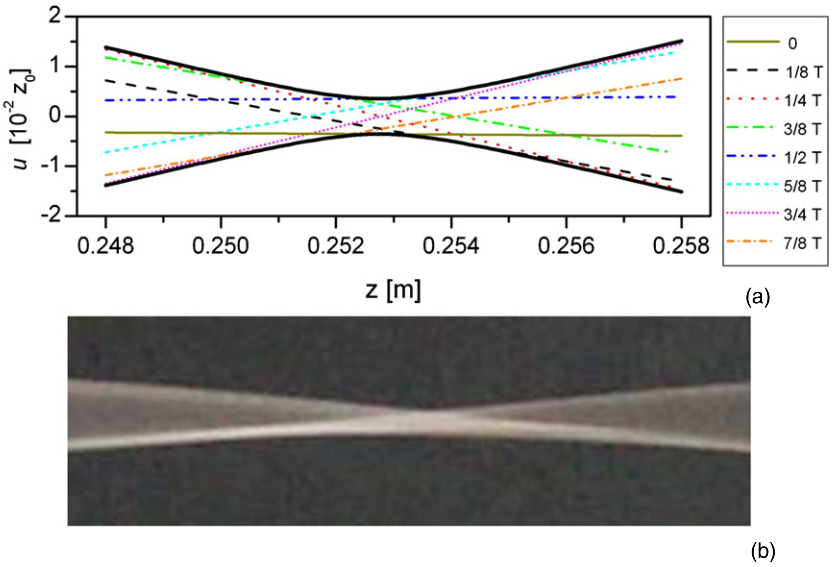

Figure 7. Behaviour of the beam in the neighbourhood of the first node for the third natural mode. (a) Theoretical solutions for times separated by 1/8 T and (b) enlargement of the photograph seen in figure 6.

Finally, on the left-hand side of figure 6, we show photographs of the first four normal modes of beam vibration and, on the right-hand side, graphics of the theoretical solutions (3.9) for $\gamma = 2\,\mathrm{s}^{-1}$ and $z_0\omega =$ constant. The experimental and simulated shapes of the beam match well in each mode, and furthermore, there are coincidences in the positions of the nodes and in the decrease of the amplitude of the antinodes with increasing distance from the forced end.

It is interesting to observe the behaviour of the nodes in both the experiment and the theoretical solutions. Figure 7(a) shows the displacement of the beam, obtained from (3.9) for different times separated by 1/8 of the period, in the neighbourhood of the first node for the third natural mode, at $z \sim 0.253$ m. Figure 7(b) is an enlargement from the photograph seen in figure 6. The amplitude of the oscillation is different than zero, which is why this is called a 'pseudo-node'.

6. Conclusion

In this paper, we show, through simple experiments at various frequencies, the response of a cantilever beam subjected to single-ended transverse vibrations. This response was successfully modelled with a theoretical solution that includes the presence of damping. Gravitational effects were also investigated and found to mainly influence the system's response to the fundamental frequency of oscillation. The hypothesis that the device supplies a constant power was confirmed and, finally, we show and discuss the presence of 'pseudo-nodes' in the normal modes of oscillation.

Acknowledgment

The authors would like to thank Dr Michael G Stout for his careful reading of the paper.

References

[1] Weaver W, Timoshenko S P and Young D H 1990 *Vibrations Problems in Engineering* 5th edn (New York: Wiley)
[2] Bert C W and Clary R R 1974 *Composite Materials: Testing and Design 3rd conf.* (Spec Tech Publication 549) (Philadelphia, PA: ASTM) pp 250–65
[3] Cheng Y F 1977 *Fibre Sci. Technol.* **10** 23–35
[4] Maiz S, Bambilla D V, Rossita C A and Laura P A A 2007 *J. Sound Vib.* **303** 895–908
[5] Fahy F and Gardonio P 2007 *Sound and Structural Vibrations: Radiation, Transmission and Response* 2nd edn (New York: Academic)
[6] Tikhonov A N and Samarskii A A 1996 *Equations of Mathematical Physics* (New York: Dover)
[7] Landau L D and Lifshitz E M 1986 *Theory of Elasticity* 3rd edn, vol 7 (Oxford: Butterworth–Heinemann)
[8] Tong K N 1960 *The Mathematical Theory of Mechanical Vibration* (New York: Wiley)
[9] Bruus H 2001 *The theory of harmonically driven, damped silicon micro-beams* http://web-files.ait.dtu.dk/bruus/TMF/publications/books/oscbeam.pdf
[10] Asmar N H 2000 *Partial Differential Equations with Fourier Series and Boundary Value Problems* (New York: Prentice-Hall)
[11] Cottrel A H 1964 *The Mechanical Properties of Matter* (New York: Wiley)
[12] Mosca H O and Mastrícola H 2000 *Jornadas SAM 2000— IV Coloquio Latinoamericano de Fractura y Fatiga* pp 1001–8
[13] Virgin L N, Santillan S T and Holland D B 2007 *Mech. Res. Commun.* **34** 312–7